

## Phase boundary of several multicube superconducting circuits in a magnetic field of arbitrary magnitude and direction

You-Min Yi

*Department of Physics, Anhui University, Hefei, Anhui, 230039, People's Republic of China*

Chia-Ren Hu

*Center for Theoretical Physics, Department of Physics, Texas A&M University, College Station, Texas 77843-4242*

(Received 13 January 1992)

A previous study [C.-R. Hu and C.-H. Huang, *Phys. Rev. B* **43**, 7718 (1991)] of the phase boundary  $T_c(\mathbf{H})$  of a single-cube superconducting circuit in an external magnetic field  $\mathbf{H}$  of arbitrary magnitude and direction is extended here to superconducting circuits containing  $2 \times 2 \times 2$ ,  $4 \times 4 \times 4$ , and  $6 \times 6 \times 6$  cubes. For the last two cases, the study reported here is limited to the vicinity of one major peak of  $T_c(\mathbf{H})$  only, in order to limit the total computing time. However, by going up to  $6 \times 6 \times 6$  cubes, we have practically obtained the limiting behavior, in the vicinity of this major peak studied, of an  $n \times n \times n$  cube circuit as  $n \rightarrow \infty$ . This result is believed to illustrate the generic behavior of all such major peaks, which, as has been noted in the earlier work of Hu and Huang, is the most important property of such circuits for most applicational purposes.

Recently Hu and Huang<sup>1</sup> have calculated the phase boundary  $T_c(\mathbf{H})$  of a  $\mu\text{m}$ -sized cubic superconducting circuit in an external magnetic field  $\mathbf{H}$ . It was shown there that this phase boundary depends in a complex and sensitive way on both the magnitude and the direction of the external magnetic field, and that the sensitive directional dependence can potentially have practical applicational values as the basis of a  $\mu\text{m}$ -sized device, which can either determine sensitively the orientation of an instrument or another device, or detect the magnitude and direction of a weak external magnetic field. It was also pointed out there that in any such applications, using a multicube circuit will most likely improve the sensitivity of the device, when compared with the use of a single-cube circuit, much like the improvement from a double-slit interferometer to a grating. This is because the sensitive dependence of  $T_c(\mathbf{H})$  of such circuits on the magnitude and direction of the external magnetic field is simply the result of interference effects due to the multipathed nature of the superconducting pair wave function in such circuits, in analogy to the interference effects exhibited by light waves in the optical devices mentioned above. One important difference between an electron wave interference device and its optical counterpart is that the electrons are charged, and therefore the phases of the electron wave functions can be altered by changing an external magnetic field, which results in a change of the fluxes threading through the holes of any multiply connected circuit. Thus the dependence of  $T_c(\mathbf{H})$  of any such circuit on the applied magnetic field vector is basically a manifestation of the famous Aharonov-Bohm effect.<sup>2</sup>

In this paper, therefore we will extend the study of Ref. 1 to several multicube superconducting circuits in order to illustrate this trend of improved sensitivity. In order to keep the cubic symmetry of the original single-cube circuit of Ref. 1, for the purpose of facilitating compar-

ison of our current results with those presented there, we have chosen to investigate only circuits that contain  $n \times n \times n$  cubes, forming a larger cube, with  $n = 2, 4$ , and  $6$ . As is already noted in Ref. 1, only the single-cube circuit is susceptible to exact analytic solution, which was performed in Ref. 1. For any  $n \times n \times n$  cube circuits with  $n > 1$ , purely numerical approaches must be resorted to, as we have done in this work. Since the amount of computing time and effort grows steeply as  $n$  increases, we have to limit this study to  $n = 2, 4$ , and  $6$ , and for  $n = 4$  and  $6$ , we have studied the vicinity of one major peak of  $T_c(\mathbf{H})$  only. The decision to study only this much is based on the following considerations: (1) As has been already explained in Ref. 1, most likely only the vicinities of the major peaks of  $T_c(\mathbf{H})$  are important in any practical applications; (2) the behaviors of  $T_c(\mathbf{H})$  in the vicinities of all of its major peaks are expected to be very similar to one another, and so the explicit presentation of one of them should be sufficient to illustrate their generic behavior; (3) we found, somewhat unexpectedly, that the behavior of  $T_c(\mathbf{H})$  for  $n = 6$  is already quite sufficient to clearly demonstrate the limiting behavior of the same for an  $n \times n \times n$  cube circuit with  $n \rightarrow \infty$ . Of course, the numerical predictions can certainly still be improved somewhat by studying even larger  $n$  values, which should be pursued if it were indeed the precise quantitative behavior of the  $n \rightarrow \infty$  limit that we had wished to obtain as our principal goal. Actually, since no laboratories to date have been able to physically produce such a three-dimensional superconducting circuit in the size range required for exhibiting the behavior studied in Ref. 1 and here, we have thus judged that high numerical accuracy for the  $n \rightarrow \infty$  limit need not be taken as even one of the principal goals of this study, especially in view of the cost involved in computing time and effort in order to obtain it. Instead, we feel that it is the qualitative change and

the generic trend as  $n$  increases that we should concentrate on here as the most important goal of this study. We conclude, therefore, that what we have studied and presented in this paper should be already sufficient for this purpose. Of course, the computer programs that we have written are for general  $n$ . (As a matter of fact, it is written for the even more general case of  $n_1 \times n_2 \times n_3$  cube circuits). Thus larger values of  $n$  and/or other regions of  $T_c(\mathbf{H})$  can always be investigated in the future using these programs when the need arises.

The theoretical foundation underlying the calculation of the mean-field transition temperature  $T_c(\mathbf{H})$  of a superconducting network was laid in the works of de Gennes<sup>3</sup> and Alexander.<sup>4</sup> It has already been extensively reviewed in many previous works including Ref. 1. (See Refs. 1 and 2 cited in Ref. 1 for many earlier experimental and theoretical references, respectively, in this area.<sup>5-7</sup>) Thus we shall be very brief and mention below only the points specific to this calculation: By an  $n \times n \times n$  cube circuit we mean a circuit made of many one-dimensional superconducting wire segments, all of equal length  $a$  and cross-sectional area—the lateral dimensions of the wires are assumed to be small compared with the temperature-dependent Ginzburg-Landau coherence length  $\xi(T)$  of the superconducting material used to make the wire segments. These wire segments should be arranged in horizontal east-west, horizontal north-south, and vertical directions—all of which will be called links—joined at many nodes, in order to form a three-dimensional wire framework. The structure should form  $n^3$  cubes sharing nodes, edges, and faces between neighboring cubes, and is in the shape of a larger cube. It has  $(n+1)^3$  nodes denoted as  $(i_1, i_2, i_3)$ , with each index  $i_\nu$  (with  $\nu=1, 2$ , and  $3$ ) running from  $0$  to  $n$ . The superconducting pair-wave-function order parameter at these nodes will be denoted as  $\Delta_{(i_1, i_2, i_3)}$ , and together they form the  $(n+1)^3$  components of a complex vector  $\Delta$ . At temperature  $T=T_c(\mathbf{H})$  these order-parameter values are all infinitesimal, and are governed by a single linear matrix equation. Writing this matrix equation as

$$\underline{M}\Delta=0, \quad (1)$$

the matrix  $\underline{M}$  must be  $(n+1)^3 \times (n+1)^3$  dimensional. (That is, for  $n=2$  it is  $27 \times 27$ , for  $n=4$  it is  $125 \times 125$ , and for  $n=6$  it is  $343 \times 343$ , but for  $n=8$ —a case we did not study—it would be  $729 \times 729$ ). The elements of  $\underline{M}$  are as follows: The diagonal matrix element  $\underline{M}_{(i_1, i_2, i_3), (i_1, i_2, i_3)}$  has the value  $-z_{(i_1, i_2, i_3)}\lambda$ , where  $\lambda \equiv \cos[a/\xi(T)]$ . The parameter  $z_{(i_1, i_2, i_3)}$  is the number of nearest-neighbor nodes of the node  $(i_1, i_2, i_3)$ , and is equal to 3 for a corner node (i.e., when all indices  $i_\alpha$  are equal to 0 or  $n$ ); to 4 for any edge node (i.e., when only two of the three indices are equal to 0 or  $n$ ); to 5 for any face node (i.e., when only one of the three indices is equal to 0 or  $n$ ); and to 6 for any interior node (i.e., when none of the three indices is equal to 0 or  $n$ ). The off-diagonal matrix element  $\underline{M}_{(i_1, i_2, i_3), (j_1, j_2, j_3)}$  is nonzero only if the nodes at  $(i_1, i_2, i_3)$  and  $(j_1, j_2, j_3)$  are nearest neighbors. That is, only when

$$|i_1 - j_1| + |i_2 - j_2| + |i_3 - j_3| = 1$$

is satisfied. The precise values of the nonvanishing off-diagonal matrix elements are dependent on the gauge chosen to represent the external magnetic field. The magnetic field is in an arbitrary direction relative to the circuit, so it will be written as  $\mathbf{H} = H(n_x \hat{\mathbf{e}}_x + n_y \hat{\mathbf{e}}_y + n_z \hat{\mathbf{e}}_z)$ , where  $n_x = \sin\alpha \cos\beta$ ,  $n_y = \sin\alpha \sin\beta$ , and  $n_z = \cos\alpha$  are the directional cosines measured relative to the three principal directions of the cubic circuit, and  $(\alpha, \beta)$  is a polar representation of the direction of the magnetic field vector. The gauge is chosen such that the vector potential  $\mathbf{A}$  has components  $A_x = Hzn_y$ ,  $A_y = H(xn_z - zn_x)$ , and  $A_z = 0$ . In this gauge the nonvanishing off-diagonal matrix element  $\underline{M}_{(i_1, i_2, i_3), (j_1, j_2, j_3)}$  has the form

$$\exp\{i\gamma[i_3 n_y(i_1 - j_1) + (i_1 n_z - i_3 n_x)(i_2 - j_2)]\}, \quad (2)$$

subject to

$$|i_1 - j_1| + |i_2 - j_2| + |i_3 - j_3| = 1,$$

and  $\gamma \equiv 2\pi\Phi/\Phi_0$ , with  $\Phi \equiv Ha^2$ , and  $\Phi_0 \equiv hc/2e$  being the flux quantum.

The temperature-dependent coherence length  $\xi(T)$  depends on  $T$  as  $\xi(0)(1 - T/T_{c0})^{-1/2}$ , where  $T_{c0}$  is the zero-field transition temperature of the superconducting material used, as well as that of the circuit. Thus to calculate the field-dependent transition temperature  $T_c(\mathbf{H})$  of the circuit, one should solve for the largest value of  $\lambda$  which can allow Eq. (1) to have a nontrivial solution. [Note that Eq. (1) has the form  $\underline{M}'\Delta = \lambda\underline{D}\Delta$ , where  $\underline{M}'$  has only the off-diagonal matrix elements of  $\underline{M}$ , whereas  $\underline{D}$  is a diagonal matrix, but not an identity matrix. Thus Eq. (1) is a generalized eigenvalue equation.] We solve this equation by starting at  $\lambda=1$  (corresponding to  $T=T_{c0}$ ), which provides an upper bound to  $\lambda$  at all  $\mathbf{H}$ , and gradually lowering  $\lambda$  until the first root of  $\det\underline{M}$  is found. We find that the larger the value of  $n$ , the easier it is to miss this first root, especially when the first two or more roots are exactly or nearly degenerate. For such cases it becomes particularly easy to skip these roots, and to land on the next lower one, which, of course, gives a false  $T_c$  that is too low. We have not searched for better approaches to handle this problem, since we find that with sufficient care we can uncover and remove all such false solutions with the present approach. The calculation of  $\det\underline{M}$  is by a standard method, so we can omit its details, and proceed directly to the presentation of the results.

We first present our results for  $n=2$ —a case we have studied in more detail because it does not cost us much computing time and effort, and it allows us to present results in parallel to the results of Ref. 1 in order to facilitate comparison of the two circuits. In Figs. 1–3, the  $\alpha$  dependence of  $(a/\xi)^2 \propto (1 - T_c/T_{c0})$  is plotted for three values of  $\beta$ , viz.,  $0$ ,  $\tan^{-1}(\frac{1}{3}) = 18.43^\circ$ , and  $45^\circ$ , and each for six values of  $\Phi/\Phi_0$ , viz.,  $\frac{1}{4}$ ,  $\frac{1}{2}$ ,  $\frac{3}{4}$ ,  $1$ ,  $2$ , and  $5$ . (As has been explained in Ref. 1, we do not need to go beyond  $90^\circ$  in  $\alpha$ , and  $45^\circ$  in  $\beta$ , for any circuit that has a cubic symmetry. As a matter of fact, all qualitative features in Figs. 2–11 of Ref. 1 associated with the cubic symmetry of the

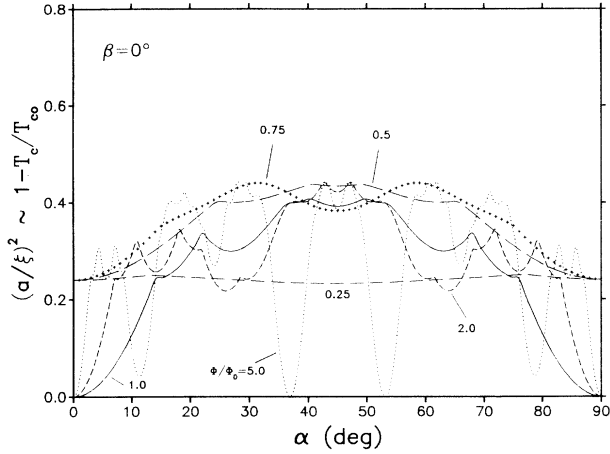


FIG. 1. Plot of  $(a/\xi)^2 \propto (1 - T_c/T_{c0})$  for a  $2 \times 2 \times 2$  cube superconducting circuit as a function of  $\alpha$  for  $\beta = 0$  and for six values of  $\Phi/\Phi_0$ , viz.,  $\frac{1}{4}$ ,  $\frac{1}{2}$ ,  $\frac{3}{4}$ , 1, 2, and 5. This figure should be compared with Figs. 2 and 7 of Ref. 1, which are for a single-cube superconducting circuit.

single-cube circuit studied there are also present in the present plots of Figs. 1–3, as they should be, since a  $2 \times 2 \times 2$  cube circuit has a cubic symmetry also.)

The chosen values for  $\beta$  and  $\Phi/\Phi_0$  in the present Figs. 1–3 form a subset of the choices in Figs. 2–11 of Ref. 1, so the readers can compare the corresponding curves presented in these two sets of figures in order to obtain some feeling on the effect of increasing  $n$  from 1 to 2, i.e., from a single-cube circuit to a  $2 \times 2 \times 2$  cube circuit. More precisely, one should compare Figs. 2 and 7 of Ref. 1 with Fig. 1 here, Figs. 4 and 9 of Ref. 1 with Fig. 2 here, and Figs. 4 and 11 of Ref. 1 with Fig. 3 here. One can see from this comparison that, except for the appearance of additional minor features as well as splittings of some peaks in  $(1 - T_c/T_{c0})$  (or troughs in  $T_c/T_{c0}$ ), the general behavior is basically the same in the corresponding curves for the two circuits. This is not surprising since the basic interference paths of the single-cube circuit

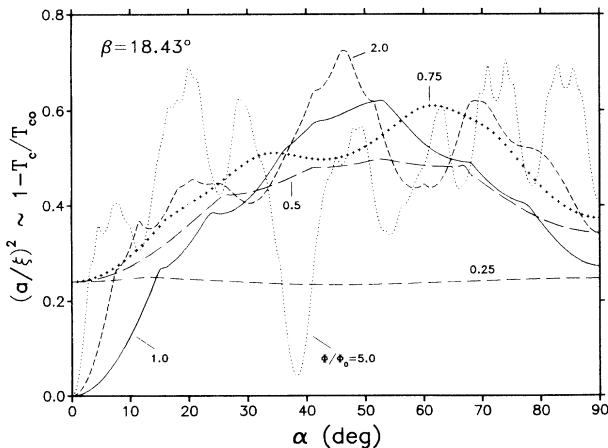


FIG. 2. Same as Fig. 1 except that  $\beta = \tan^{-1}(\frac{1}{3}) = 18.43^\circ$ . This figure should be compared with Figs. 4 and 9 of Ref. 1.

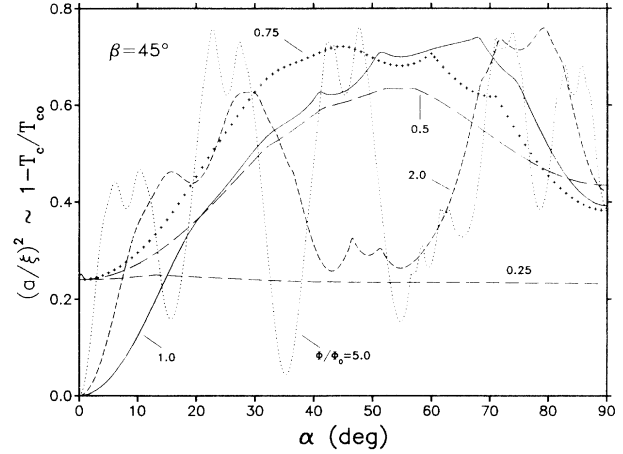


FIG. 3. Same as Fig. 1 except that  $\beta = 45^\circ$ . This figure should be compared with Figs. 6 and 11 of Ref. 1.

are also present in any multicube circuits, whereas the reverse is not true. (The splitting of the troughs in  $T_c/T_{c0}$  is clearly due to the appearance of additional minor peaks caused by constructive interference between those interference paths which enclose larger areas, and therefore they can appear where a minimum used to be.) It is important to note here, however, that an important qualitative change due to the increase of  $n$  is not revealed clearly in these plots, and it will be made clear only when we present Figs. 6 and 7, but first we will present Figs. 4

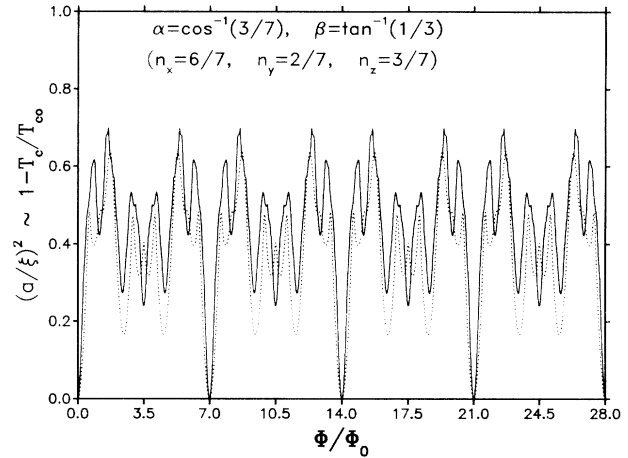


FIG. 4. The solid line is a plot of  $(a/\xi)^2 \propto (1 - T_c/T_{c0})$  for a  $2 \times 2 \times 2$  cube superconducting circuit as a function of  $\Phi/\Phi_0$ , for the special choice of the polar angles  $\alpha$  and  $\beta$  as given, which is such that the directional cosines of the applied magnetic field are in the rational ratios 6:2:3. This curve should be compared with the dotted line, which is reproduced from Fig. 12 of Ref. 1, and is the corresponding plot for a single-cube superconducting circuit. Both curves are seen to be periodic with the same period 7, essentially because if a single-cube circuit is not frustrated at all at a certain applied magnetic field (vector), then so must be any multicube circuit of the same elementary cube dimension. However, the detailed minor features in the solid curve are different from those in the dotted curve as expected, because a  $2 \times 2 \times 2$  cube superconducting circuit has more interference paths than a single-cube circuit.

and 5 in order to complete our comparison with Ref. 1: In these two figures we compare the  $\Phi/\Phi_0$  dependence of  $(a/\xi)^2 \propto (1 - T_c/T_{c0})$  for a  $2 \times 2 \times 2$  cube circuit and a single-cube circuit, at two special choices of the directions of  $\mathbf{H}$ . These two choices of the directions of  $\mathbf{H}$  are exactly those made in the Figs. 12 and 13 of Ref. 1, and so we can directly transfer the results in those two figures into the present two figures as dotted lines, whereas the solid lines in these figures are the corresponding results calculated here for a  $2 \times 2 \times 2$  cube circuit. (We will not make a similar comparison with the Fig. 14 of Ref. 1, because that case is not much different from the second case studied here.) Thus in Fig. 4 the polar angles of  $\mathbf{H}$  are fixed at  $\alpha = \cos^{-1}(\frac{2}{3})$ , and  $\beta = \tan^{-1}(\frac{1}{3})$ , giving the directional cosines  $n_x = \frac{6}{7}$ ,  $n_y = \frac{2}{7}$ , and  $n_z = \frac{3}{7}$ , which are all in rational ratios. For this choice  $T_c$  can rise to  $T_{c0}$ , and therefore  $(a/\xi)^2 \propto (1 - T_c/T_{c0})$  can drop to zero, whenever  $\Phi/\Phi_0$  is equal to a multiple of 7—the common denominator of the directional cosines, since the flux components through the elementary squares in all three principal directions of any single- or multicube circuits will all be integer multiples of the flux quantum, and no frustration would be present in any closed loops in such circuits. This explains the periodic structure of period 7 in both the solid line and the dotted line plotted in this figure, but it is also clear from this figure that not all of the minor maxima and minima in the two curves are located at the same  $\Phi/\Phi_0$ , because they can arise from larger interference loops which are not all shared by the two circuits. Next, in Fig. 5 the polar angles of  $\mathbf{H}$  are fixed at  $\alpha = \cos^{-1}(\sqrt{3/8})$ , and  $\beta = \tan^{-1}(1/2)$ , giving the directional cosines  $n_x = 1/\sqrt{2}$ ,  $n_y = 1/\sqrt{8}$ , and  $n_z = \sqrt{3/8}$ , which are no longer all in rational ratios. It is then no longer possible for  $T_c$  to rise to  $T_{c0}$  at any finite value of  $H$  or  $\Phi/\Phi_0$ , and the curves plotted are then no longer periodic. Nevertheless, the solid line and the dotted line

show much similarity, in the sense that all of the major dips in these two curves are located at the same values of  $H$  or  $\Phi/\Phi_0$ . These minima must have arisen from the same interference paths which exist in both circuits. Of course some minor minima and maxima in these two curves do not happen at the same  $\Phi/\Phi_0$ , and the solid curve has more fine structure than the dotted curve, for the same reason as has been given above in association with the similar features in the two curves plotted in Fig. 4.

The comparisons made in Figs. 4 and 5 lead us to essentially the same conclusion as the comparisons made in Figs. 1–3, viz., in order to clearly reveal the qualitative change and the general trend as  $n$  increases, we need to go to the next two plots: Figs. 6 and 7. In these figures we concentrate on the vicinity of one isolated major peak of  $T_c/T_{c0}$  [i.e., one major minimum in  $(a/\xi)^2 \propto (1 - T_c/T_{c0})$ ], and study it in detail. We choose to study the same peak the vicinity of which was presented in a three-dimensional plot in Fig. 15 of Ref. 1. This peak corresponds to  $\Phi/\Phi_0 = 14$ ,  $\alpha = \cos^{-1}(\frac{2}{3}) \approx 64.62^\circ$ , and  $\beta = \tan^{-1}(\frac{1}{3}) \approx 18.43^\circ$ . Here we choose to not present a three-dimensional plot, but to present two two-dimensional cross-sectional plots, in order to reveal more quantitative details. In Fig. 6, we hold  $\beta = \tan^{-1}(\frac{1}{3})$  constant, and plot  $(a/\xi)^2$  against  $\alpha$  over a  $10^\circ$  range covering the point  $\alpha = \cos^{-1}(\frac{2}{3})$ . In Fig. 7, we hold instead  $\alpha = \cos^{-1}(\frac{2}{3})$  constant, and plot  $(a/\xi)^2$  against  $\beta$  over a  $10^\circ$  range covering the point  $\beta = \tan^{-1}(\frac{1}{3})$ . Together they reveal the detailed behavior of a single, major, three-dimensional peak of  $T_c(\alpha, \beta)$  [shown as a major minimum of  $(a/\xi)^2 \propto (1 - T_c/T_{c0})$ ]. In these two figures, we have not only presented our result for  $n = 2$ , but we have extended our calculation to  $n = 4$  and  $n = 6$  as well, and we have also presented in these figures our earlier result for  $n = 1$ , so that an important qualitative trend as  $n$  in-

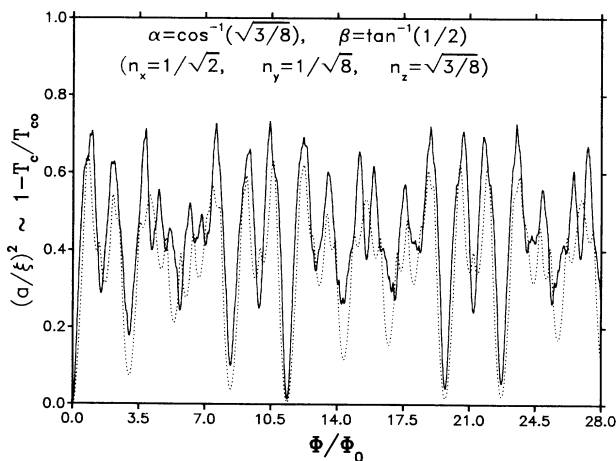


FIG. 5. Same as Fig. 4 except that the directional cosines are now in the partially rational ratios  $2:1:\sqrt{3}$ . Again the solid line should be compared with the dotted line, which is reproduced from Fig. 13 of Ref. 1. Note that the beatlike structure in that figure is slightly less visible in this figure, although it should still be present according to theoretical understanding, probably because of the more complex dependence of  $T_c$  on the magnetic field for the present case.

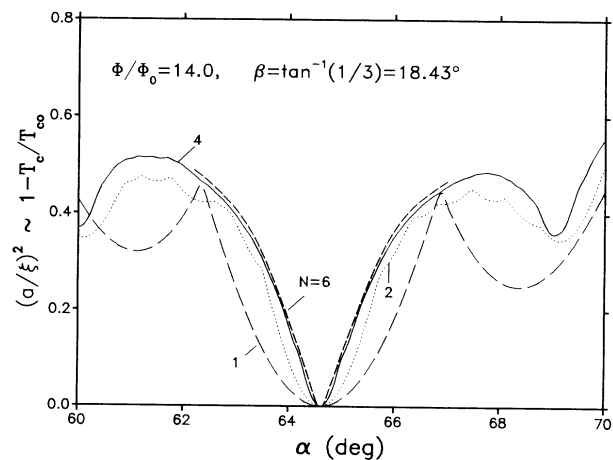


FIG. 6. Plot of  $(a/\xi)^2 \propto (1 - T_c/T_{c0})$  of  $n \times n \times n$  cube superconducting circuits, with  $n = 1, 2, 4$ , and  $6$ , as a function of  $\alpha$  in a  $10^\circ$  range covering the point  $\alpha = \cos^{-1}(\frac{2}{3}) \approx 64.62^\circ$ , for fixed values of  $\beta = \tan^{-1}(\frac{1}{3}) \approx 18.43^\circ$  and  $\Phi/\Phi_0 = 14$ . The only major dip in this figure corresponds to the major peak located near the center of Fig. 13 of Ref. 1. Important additional comments about this figure are given in the caption for Fig. 7.

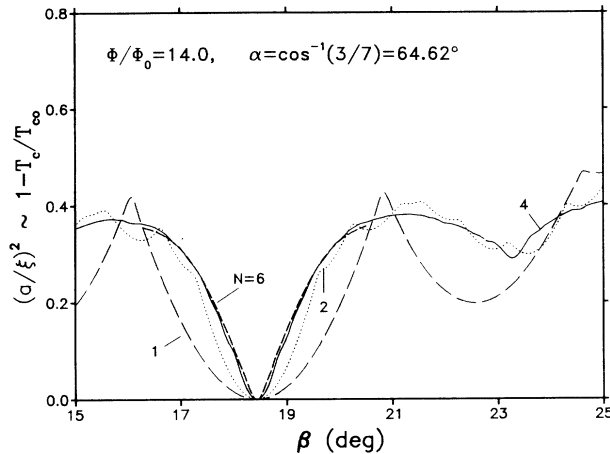


FIG. 7. Same as Fig. 6 except that this time  $\alpha$  is held fixed at  $\cos^{-1}(3/7) \approx 64.62^\circ$ , and  $\beta$  is varied through a  $10^\circ$  range covering the point  $\beta = \tan^{-1}(1/3) \approx 18.43^\circ$ . This figure and Fig. 6 together provide two cutout views of a three-dimensional profile of a major peak of  $T_c(\mathbf{H})$  as a function of the two polar angles  $\alpha$  and  $\beta$  describing the direction of the magnetic field  $\mathbf{H}$ , with the magnitude of  $\mathbf{H}$  held at one of the special values for which a major peak of  $T_c$  can be obtained at certain values of  $\alpha$  and  $\beta$ . (These values are given in the caption of Fig. 6) The curves plotted in these two figures reveal the gradual change of the profile of this major peak as  $n$  is increased from 1 toward infinity, i.e., from a single-cube superconducting circuit toward an infinite, three-dimensional, cubic superconducting network. This behavior is believed to be generic among all major peaks of  $T_c(\mathbf{H})$  of such circuits.

creases can be clearly revealed here: Namely, a typical major peak of  $T_c/T_{c0}$  will change from being round and paraboloidlike at  $n=1$  to becoming more and more pointed and cone-shaped as  $n$  increases. As a matter of fact, it is clear from these two figures that the result for  $n=6$  has essentially revealed the limiting behavior of an  $n \times n \times n$  cube circuit with  $n \rightarrow \infty$ , namely the  $T_c(\alpha, \beta)$  surface will be rather smooth at its troughs (contrary to the low- $n$  cases where the troughs will show v-shaped valleys—see Fig. 15 of Ref. 1), whereas its major maxima will be cone-shaped, with pointed tips, as we have already noted. This change of the qualitative behavior of the major peaks of  $T_c(\mathbf{H})$  is already projected in Ref. 1 based on our knowledge of two-dimensional circuits and networks, but it is explicitly confirmed here. This confirmation is very important since any applications of such circuits will most likely be relying only on the behavior of their  $T_c(\mathbf{H})$  near one of such major peaks—see Ref. 1 for elaboration of this point—and a pointed cone-shaped peak will mean that the value of  $T_c(\mathbf{H})$  will drop *linearly* with the deviation of the magnitude and direction of the external magnetic-field vector from the optimum values to set  $T_c$  at one of such peak values, instead of *quadratically* as for the low- $n$  circuits. This clearly can improve the sensitivity of any device that is based on the major-peak behavior

of  $T_c(\mathbf{H})$  of such circuits, as we have asserted in the beginning of this paper based on the analogy with the behavior of double-slit interferometers and gratings. However, the analogy clearly cannot carry us as far as we have done here with an explicit calculation. For example, the analogy clearly does not allow us see this quadratic-to-linear change of the dependence of  $T_c(\alpha, \beta)$  of such circuits at any of its major peaks as  $n$  is increased from 1 to  $\infty$ . Another point strongly suggested by the results of this study—although we did not provide a rigorous proof—is that the phase boundary  $T_c(\mathbf{H})$  of an *infinite three-dimensional* superconducting network is a continuous *fractal* hypersurface in four dimensions, i.e., in the space of  $(T_c, H_x, H_y, H_z)$  or  $(T_c, H, \alpha, \beta)$ . This conclusion is actually an expected generalization of the well-known result for some time that the phase boundary  $T_c(H)$  of a *two-dimensional* infinite superconducting network in a perpendicular magnetic field  $H$  is a continuous fractal curve with self-similar structures.<sup>4,8</sup>

In summary, we have in this work extended a previous calculation of the phase boundary  $T_c(\mathbf{H})$  of a single-cube superconducting circuit to several multicube superconducting circuits in the overall shape of a larger cube. Our results have quantified an earlier qualitative projection made in Ref. 1 which was based on an analogy: Namely, the major peaks of  $T_c(\mathbf{H})$  of a  $n \times n \times n$  cube superconducting circuits will become more and more cone shaped with a pointed tip if  $n$  is increased to approach infinity, in contrast with the major peaks of a small- $n$  circuit which are round and paraboloidlike. This means that for such large- $n$  circuits,  $T_c(\mathbf{H})$  will drop essentially linearly from its peak value of  $T_{c0}$  as either the magnitude or the direction of the applied magnetic-field *vector* is moved slightly away from their optimal values which preset the  $T_c(\mathbf{H})$  of such a circuit to one of its major peak values. (That a magnitude change from such an optimal value can produce such a change was already revealed in previous studies of two-dimensional circuits and networks.<sup>4,8</sup>) This property should imply high sensitivity for device applications of such large- $n$  circuits to determine the orientation of an instrument, or to measure the magnitude and direction of an external weak magnetic field. Note that in a known nonuniform external magnetic field, such circuits can in principle also be used to determine sensitively position in three-dimensional space, although this last potential application may not be as practical as the other applications suggested. As far as physics is concerned, what we have studied here is an interesting way to exhibit the Aharonov-Bohm effect. Our results also establish with reasonable certainty that the phase boundary  $T_c(\mathbf{H})$  of an infinite three-dimensional superconducting network is a continuous *fractal* hypersurface in a four-dimensional space.

One of us (C.R.H.) would like to acknowledge partial support from the Texas Center for Superconductivity at the University of Houston.

<sup>1</sup>C.-R. Hu and C.-H. Huang, *Phys. Rev. B* **43**, 7718 (1991).

<sup>2</sup>Y. Aharonov and D. Bohm, *Phys. Rev.* **115**, 485 (1959).

<sup>3</sup>P. G. de Gennes, *C. R. Acad. Sci. Ser. B* **292**, 9 (1981); **292**, 279 (1981).

<sup>4</sup>S. Alexander, *Phys. Rev. B* **27**, 1541 (1983).

<sup>5</sup>Some additional experimental references on the subject of superconducting networks not cited in Ref. 1 are the following: Y. Y. Wang, B. Doucot, R. Rammal, and B. Pannetier, *Phys. Lett. A* **119**, 145 (1986); P. Gandit, J. Chaussy, B. Pannetier, A. Vareille, and A. Tissier, *Europhys. Lett.* **3**, 623 (1987); Y. Y. Wang, R. Steinmann, J. Chaussy, R. Rammal, and B. Pannetier, *Jpn. J. Appl. Phys.* **26**, Suppl. 26-3 (1987); J. M. Gordon and A. M. Goldman, *Phys. Rev. B* **35**, 4909 (1987); J. M. Gordon, A. M. Goldman, and B. Whitehead, *Phys. Rev. Lett.* **59**, 2311 (1987); G. S. Grest, P. M. Chaikin, and D. Levine, *ibid.* **60**, 1162 (1988); S. P. Benz, M. G. Forrester, M. Tinkham, and C. J. Lobb, *Phys. Rev. B* **38**, 2869 (1988); P. Santhanam and C. C. Chi, *Physica B* **152**, 129 (1988); Y. Y. Wang, B. Pannetier, and R. Rammal, *J. Phys. (Paris)* **49**, 2045 (1988); R. G. Steinmann and B. Pannetier, *Europhys. Lett.* **5**, 559 (1988); Xiao-Dun Jing and Zhao-Qing Zhang, *Phys. Rev. B* **40**, 4384 (1989); O. Buisson, M. Giroud, and B. Pannetier, *Europhys. Lett.* **12**, 727 (1990); B. Pannetier, O. Buisson, P. Gandit, Y. Y. Wang, J. Chaussy, and R. Rammal, *Surf. Sci.* **2229**, 331 (1990); M. A. Itzler, A. M. Behrooz, C. W. Wilks, R. Bojko, and P. M. Chaikin, *Phys. Rev. B* **42**, 8319 (1990); F. Yu, A. M. Goldman, R. Bojko, C. M. Soukoulis, Q. Li, and G. S. Grest, *ibid.* **42**, 10536 (1990); C. W. Wilks, R. Bojko, and P. M. Chaikin, *ibid.* **43**, 2721 (1991); H. J. Fink, O. Buisson, and B. Pannetier, *ibid.* **43**, 10144 (1991); F. Yu, N. E. Israeloff, A. M. Goldman, and R. Bojko, *Phys. Rev. Lett.* **68**, 2535 (1992).

<sup>6</sup>Some additional theoretical references on the subject of superconducting networks not cited in Ref. 1 are the following: R.

Rammal and J. Angles d'Auric, *J. Phys. C* **16**, 3933 (1983); T. C. Halsey, *Phys. Rev. B* **31**, 5728 (1985); R. Rammal, T. C. Lubensky, and G. Toulouse, *J. Phys. (Paris) Lett.* **44**, L65 (1983); R. Young, *Phys. Rev. B* **31**, 4294 (1985); H. J. Fink and A. López, *J. Phys. (Paris) Lett.* **46**, L961 (1985); Y. Y. Wang, B. Doucot, R. Rammal, and B. Pannetier, *Phys. Lett. A* **119**, 145 (1986); Y. Y. Wang, R. Rammal, and B. Pannetier, *J. Low-Temp. Phys.* **68**, 301 (1987); Y. Park, J. Kim, and D. Kim, *Phys. Rev. B* **38**, 741 (1988); H. J. Fink, D. Rodrigues, and A. López, *ibid.* **38**, 8767 (1988); F. Nori and Q. Niu, *Physica B* **152**, 105 (1988); Y. Y. Wang, B. Pannetier, and R. Rammal, *J. Phys. (Paris)* **49**, 2045 (1988); Q. Niu and F. Nori, *Phys. Rev. B* **39**, 2134 (1989); B. Jeanneret, Ph. Flückiger, J. L. Gavilano, Ch. Leemann, and P. Martinoli, *ibid.* **40**, 11374 (1989); C. C. Chi, P. Santhanam, and P. E. Blöchl, *ibid.* **42**, 76 (1990); H. S. J. van der Zant, M. N. Webster, J. Romijn, and J. E. Mooij, *ibid.* **42**, 2647 (1990); L. L. Daemen and J. E. Gubernatis, *ibid.* **43**, 413 (1991); **43**, 2625 (1991); R. A. Ferrell, *ibid.* **43**, 2726 (1991); A. I. M. Rae, *ibid.* **43**, 2956 (1991); S. N. Sun and J. P. Ralston, *ibid.* **43**, 5375 (1991); H. J. Fink, O. Buisson, and B. Pannetier, *ibid.* **43**, 10144 (1991); H. J. Fink and S. B. Haley, *ibid.* **43**, 10151 (1991).

<sup>7</sup>For an excellent, but already dated, review on the subject of superconducting networks, see: B. Pannetier, in *Quantum Coherence in Mesoscopic Systems*, NATO ASI Series, edited by B. Kramer (Plenum, New York, 1991), p. 457. See also the *Proceedings of the NATO Advanced Research Workshop on Coherence in Superconducting Networks, Delft, 1987*, edited by J. E. Mooij and G. B. J. Schön [*Physica B* **152** (1988)].

<sup>8</sup>R. Rammal, T. C. Lubensky, and G. Toulouse, *Phys. Rev. B* **27**, 2820 (1983); B. Pannetier, J. Chaussy, R. Rammal, and J. C. Villegier, *Phys. Rev. Lett.* **53**, 1845 (1984). See also, C.-R. Hu and R. L. Chen, *Phys. Rev. B* **37**, 7907 (1988).